

## FIXED GRID FINITE ELEMENT ANALYSIS OF SOLIDIFICATION

Jerzy Banaszek\*, Marek Rebow\* and Tomasz A. Kowalewski\*\*

\*Institute of Heat Engineering, Warsaw University of Technology, PL 00-665 Warsaw

\*\*Center of Mechanics, IPPT PAN, PL 00-049 Warsaw, Poland

**ABSTRACT.** A semi-implicit operator splitting technique is combined with an enthalpy-porosity method to solve both isothermal and temperature range solidification on equal- and unequal-order finite element grids. The performance of the presented algorithm is studied by solving some benchmark problems including a driven cavity flow, free convection (with and without Boussinesq approximation) and a binary alloy solidification. Solutions obtained are free from wiggles and spurious pressure modes and they fit fairly well to the results reported by others. More comprehensive analysis of the algorithm's accuracy is given by comparing the obtained results with both the boundary-fitted finite difference front tracking solution and experimental data for the freezing of water in the differentially heated square cavity. Although the calculated volume of the ice meshes well with the experimental data, the detailed structure of flow does not. Possible explanations for this incongruity are discussed in the body of this paper.

### INTRODUCTION

Naturally occurring substances, as well as materials used in engineering applications, almost always exist in the form of a multi-constituent system (e.g. alloys). The presence of a binary component within a material alters the nature of the solid-liquid phase transition. The ability to predict the behaviour of the binary system during solid-liquid phase change is of formidable value to engineering and accurate understanding and control of this phenomenon is critical to the improvement and refinement of many technological processes.

The primary difficulty in analysis of such systems is that the nature of the interface movement, latent energy transfer and convection mechanisms, introduces non-linearity in the governing equations. Therefore, despite a large number of relevant papers published recently, developing numerical algorithms for these complex problems that are robust, computationally efficient and geometrically versatile, is still a considerable challenge, particularly in the FEM context.

The first and crucial step is to develop reliable 2-D numerical models and their algorithms which simulate heat, mass and momentum transfer in both isothermal and temperature-range solid-liquid phase change. To include the effect of free convection in a liquid and a mushy regions, the whole set of coupled momentum, energy and mass balance equations has to be solved simultaneously. However, poor computational efficiency of the simultaneous solution approach, commonly used in the early FEM analysis of incompressible fluids<sup>1</sup>, is a major impediment in the widespread use of FEM in computational fluid dynamics. Therefore, special sophisticated acceleration techniques and algorithms have been developed to speed up FEM calculations. Most of them takes their origin from finite difference calculations. To decouple the continuity and momentum equations for incompressible fluids, Chorin has developed the fractional step method<sup>2,3</sup>. The momentum equation is first solved disregarding the pressure gradient term. Then, the provisional velocity field, thus obtained, is corrected by taking into account the pressure contribution through the enforcement of the incompressibility requirement.

In recently developed operator splitting techniques, the discrete diffusion-convection terms of momentum and energy equations are split according to physical processes and the contribution from each of these processes (i.e., convection and diffusion), is calculated separately in the time integration procedure. Ramaswamy<sup>4</sup> has reported the successful use of one such technique where the convective terms of momentum and energy equations are integrated in time using the second order Adams Bashforth scheme, whereas the diffusive terms are calculated using the backward Euler scheme.

To develop a robust and computationally efficient algorithm of the Galerkin FEM for viscous incompressible fluids we use the Chorin's fractional step method<sup>2,3</sup>, the semi-implicit operator splitting procedure of Ramaswamy and Jue<sup>4</sup> and the segregation solution technique. In the latter technique, which takes its origin from the SIMPLE-like FDM algorithms<sup>5</sup>, at each iteration step linearized momentum equations are solved sequentially and independently. Then, the provisional velocity components are corrected by solving the Poisson pressure equation (resulting from Chorin's method). An un-equal-order velocity-pressure interpolation<sup>1</sup> has been applied in calculations to avoid spurious pressure modes in FEM solution. Velocity field has been interpolated within an element by the bi-quadratic Lagrange polynomial; pressure by the bi-linear one.

A thus developed algorithm and its computer code have been further extended to include free convection and phase change phenomena. The commonly used enthalpy formulation of phase-change problems enables to solve a moving boundary problem on a fixed grid - without the need for any detailed knowledge about transport conditions at the interface. It accounts for the latent heat evolution through the use of the total enthalpy concept that includes both sensible heat and liberated heat in one dependent variable. Among different variants of the enthalpy approach, the so-called general source-based method developed by Voller and Swaminathan<sup>6</sup> for conduction driven phase change, seems to be the most effective one as it performs equally well in both isothermal and temperature-range phase change models. Therefore, the method has been extended to calculate convective transfer of the latent heat effects and then adapted in the algorithm. In the temperature-range solidification of a binary system three different zones can be distinguished - a solid region, a liquid one and a mushy zone. At the liquid/solid interface the liquid velocity should take zero value, whereas in the mushy zone it should gradually decrease as the solid volume fraction increases. Such behaviour of the velocity field in the vicinity of a sharp or dispersed phase front, can be modelled by various switch-off techniques<sup>1,7</sup>. The most physically justified approach is to assume that a mushy zone can be treated as a porous medium with porosity equal to the liquid volume fraction<sup>7</sup>. The pressure gradient is described by Carman-Kozeny law and an additional source term is added to the momentum balance equation to imitate the above described behaviour of the system in the mushy zone<sup>7</sup>.

To verify performance and accuracy of the presented algorithm some available bench-mark problems<sup>1,4,7</sup>, commonly used in comparing alternative numerical models, have been solved. They include a lid-driven cavity flow, free convection of water in the differentially heated square cavity and binary alloy solidification driven by conduction and buoyancy forces.

The robustness of the method makes it preferable for solving practical engineering problems with complex geometry and fluid properties. However, when accuracy is demanded, the freedom of the enthalpy-porosity approach, within methodology for the definition of phase change region properties, may become a drawback. To elucidate potential limitations of the method, detailed accuracy comparison is performed using experimental data<sup>8</sup> and other numerical calculations, which are obtained by using the boundary-fitted finite difference code<sup>9</sup>, for freezing of pure water in the differentially heated square cavity.

## FINITE ELEMENT MODEL AND COMPUTATIONAL ALGORITHM

The processes accompanying phase change are governed by the commonly known fundamental equations of conservation of mass (the incompressibility constraint), momentum and energy. Their weak form is obtained by using the Galerkin weighted residual method along with un-equal- or equal-order interpolations of velocity components,  $v_i$ , pressure,  $p$ , and temperature,  $T$ ,

$$v_i = N_k(v_i)_k, \quad T = N_k T_k, \quad p = M_l p_l, \quad \text{for } k = 1, 2, \dots, N_v; \quad l = 1, 2, \dots, M_p \quad (1)$$

where  $N_v$  and  $M_p$  are numbers of velocity and pressure nodes over each element, respectively.  $N_k$  represents the bi-quadratic (or bi-linear) Lagrange polynomial shape function, whereas  $M_l$  is the bi-linear Lagrange polynomial shape function. Thus, the set of equations is obtained for the semi-discrete mixed FEM

$$\left. \begin{aligned} [\mathbf{M}] \cdot \left\{ \frac{d\mathbf{v}}{dt} \right\} + [\mathbf{K}^c(\mathbf{v}) + \mathbf{K}^d] \cdot \{\mathbf{v}\} &= -[\mathbf{G}] \cdot \{p\} + \{\mathbf{F}\} \\ [\mathbf{D}] \cdot \{\mathbf{v}\} &= 0 \\ [\mathbf{C}] \cdot \left\{ \frac{dT}{dt} \right\} + [\mathbf{K}_T^c(\mathbf{v}) + \mathbf{K}_T^d] \cdot \{T\} &= \{\mathbf{F}_T\} \end{aligned} \right\} \quad (2)$$

where  $\mathbf{M}$ ,  $\mathbf{C}$ ,  $\mathbf{K}^c$ ,  $\mathbf{K}^d$ ,  $\mathbf{G}$ ,  $\mathbf{D}$  are mass, heat capacity, convective, diffusive, pressure gradient and divergence matrices, respectively.

To save computational efforts, Eqs.(2) are temporally integrated using Chorin's projection method, Adams-Bashforth scheme for the convection terms and the backward Euler scheme for the diffusion terms and for the incompressibility equation. In the first step, the linearized momentum equations with disregarded pressure terms are solved consecutively for each velocity component

$$[\mathbf{M}] \cdot \left\{ \frac{v_i^* - v_i^n}{\Delta t} \right\} + [\mathbf{K}^d] \cdot \{v_i^*\} = - \left( \frac{3}{2} [\mathbf{K}^c(\mathbf{v}^n)] \cdot \{v_i^n\} - \frac{1}{2} [\mathbf{K}^c(\mathbf{v}^{n-1})] \cdot \{v_i^{n-1}\} \right) + \{F_i^n\} \quad (3)$$

Then, the provisional velocity field  $\mathbf{v}^*$ , thus obtained, is corrected by taking into account the pressure contribution through the enforcement of the incompressibility constraint

$$\left. \begin{aligned} [\mathbf{G}^T \mathbf{M}^{-1} \mathbf{G}] \cdot \{p^{n+1}\} &= -[\mathbf{G}^T] \cdot \{\mathbf{v}^*\} / \Delta t \\ \{\mathbf{v}^{n+1}\} &= \{\mathbf{v}^*\} - \Delta t [\mathbf{M}^{-1} \mathbf{G}] \cdot \{p^{n+1}\} \end{aligned} \right\} \quad (4)$$

The right hand side vectors of the above equations result from both volumetric sources and natural boundary conditions. In the porosity model of a mushy zone volume source terms of the momentum equations have the following form

$$F_{v_1} = A v_1, \quad F_{v_2} = A v_2 + g(\rho_{\text{ref.}} - \rho) \quad (5)$$

where  $g(\rho_{\text{ref.}} - \rho)$  represents the buoyancy forces ( $g$  - gravity acceleration,  $\rho$  - density), whereas  $A = -C_p (1 - f_1)^2 / f_1^2$  is used to mimic the Carman-Kozeny law of flow in a porous medium<sup>7</sup>.  $f_1$  is a volumetric liquid fraction and  $C_p$  is a constant accounting for the porous medium morphology.

Eventually, the corrected velocity field is used to calculate temperature from the nonlinear energy balance equation. Using the total enthalpy definition for the two-phase region

$$H = (1 - f_1)H_s + f_1H_l = (1 - f_1) \int_{T_{\text{ref.}}}^T (\rho c)_s dT + f_1 \left( \int_{T_{\text{ref.}}}^T (\rho c)_l dT + \rho_l L \right) \quad (6)$$

where subscripts “l” and “s” stand for liquid and solid, respectively and  $\rho$ ,  $c$  and  $L$  are density, specific heat and specific latent heat, respectively, and assuming that the solid phase is motionless, the Kirchoff-Fourier energy balance equation can be written as

$$(\rho c) \frac{\partial T}{\partial t} + \rho v_j c_l \frac{\partial T}{\partial x_j} = \frac{\partial}{\partial x_j} \left( \lambda \frac{\partial T}{\partial x_j} \right) - \delta H(T) \frac{\partial f_l}{\partial t} \quad (7)$$

where  $\rho$ ,  $(\rho c)$  and  $\lambda$  are thermophysical properties of mixture,  $\delta H(T) = \rho_l L + ((c\rho)_l - (c\rho)_s)T$  is the difference of total enthalpy of liquid and solid at temperature  $T$ , and  $v_j$  represents a component of the apparent velocity (product of fluid velocity and mass liquid fraction). Further assuming that the volume liquid fraction is a given function of temperature, i.e.,  $f_l = F(T)$ , and modelling the latent heat evolution by the general source based method of Voller<sup>6</sup>, the iteration solution procedure is established, where at each iteration step “r” temperature and the volume liquid fraction are calculated from

$$\begin{aligned} & \left[ \mathbf{C} + \mathbf{M}_{PH} + \Delta t \mathbf{K}_T^d \right]_r \cdot \left\{ T^{n+1} \right\}_{r+1} = -\Delta t \left( \frac{3}{2} \left[ \mathbf{K}_T^c(\mathbf{v}^n) \right] \cdot \left\{ T^n \right\} - \frac{1}{2} \left[ \mathbf{K}_T^c(\mathbf{v}^{n-1}) \right] \cdot \left\{ T^{n-1} \right\} \right) + \\ & + \left[ \mathbf{M}_{PH} \right] \cdot \left\{ f_l^n - \left( f_l^{n+1} \right)_r \right\} \\ & \left\{ f_l^{n+1} \right\}_{r+1} = \left\{ f_l^{n+1} \right\}_r + \left\{ \left( \frac{dF}{dT} \right)_r \cdot \left( \left( T^{n+1} \right)_{r+1} - F^{-1} \left( f_l^{n+1} \right)_r \right) \right\} \end{aligned} \quad (8)$$

where a k-term of the diagonal phase change matrix  $(\mathbf{M}_{PH})_{kk} = \delta H(T_k) \int_{\Omega} N_k d\Omega$ .

## NUMERICAL EXAMPLES AND DISCUSSION

*Driven cavity flow.* To verify the performance of the presented algorithm for a recirculating flow, the problem of flow in a closed square cavity driven by the lid movement is considered. The lid moves with the unit velocity in its own plane. The flow is completely determined by the Reynolds number, defined for the lid velocity  $v_l$ , i.e.,  $Re = \rho v_l L / \mu$ , where  $L$  is the unit length of the lid. To compare the equal-order and unequal-order FEM interpolations, the problem was calculated on two different non-uniform grids. First, the 900 bi-linear elements for the velocity and pressure were applied. Then, the grid of 225 elements was used, where the velocity field was interpolated with the bi-quadratic Lagrange polynomials and the pressure field only with the bi-linear ones. The obtained results are given in Fig.1, where velocity components along the vertical and the horizontal centre lines of the cavity are compared for the equal-order (4/4 element) and unequal-order (9/4) interpolations. Both solutions are free from wiggles and spurious pressure modes, and they differ only slightly from each other. They also fall in with the results reported by others<sup>4</sup>.

*Free convection of water.* To examine the validity of the operator-splitting FEM method in calculating coupled heat transfer and fluid flow problems, free convection of water in the differentially heated square cavity has been solved. The temperature of the right-cold and the left-hot wall is set to 0°C and +10°C, respectively. The remaining cavity walls are assumed adiabatic. Water is the fluid that does not obey the Boussinesq approximation as its density, as well as viscosity, is a non-linear function of temperature<sup>10</sup>. In Fig. 2 the steady-state velocity and temperature fields, obtained on the grid of 40x40 equal-order finite elements, are compared with the pertinent results of the reference numerical solution, received by using the false-transient code FRECON3V<sup>12</sup> on the finite difference grid of 41x41 nodes. Satisfactory good agreement of both solutions is visible in Fig. 2.

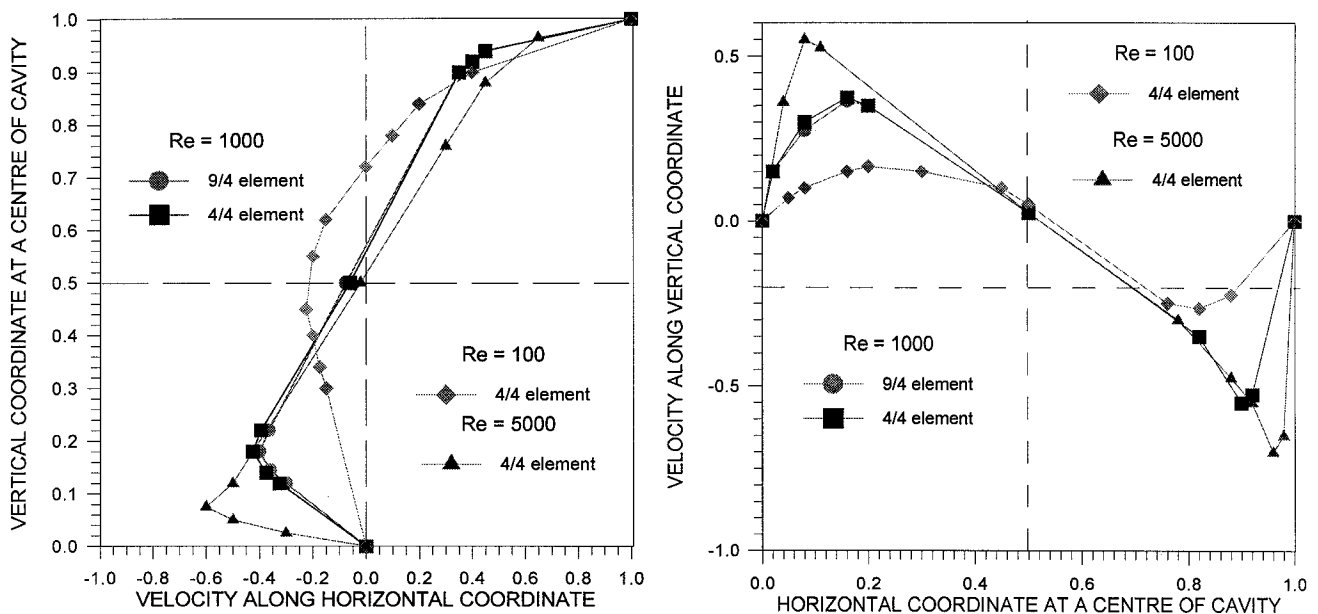


Figure 1. Velocity components along vertical and horizontal centre lines of cavity

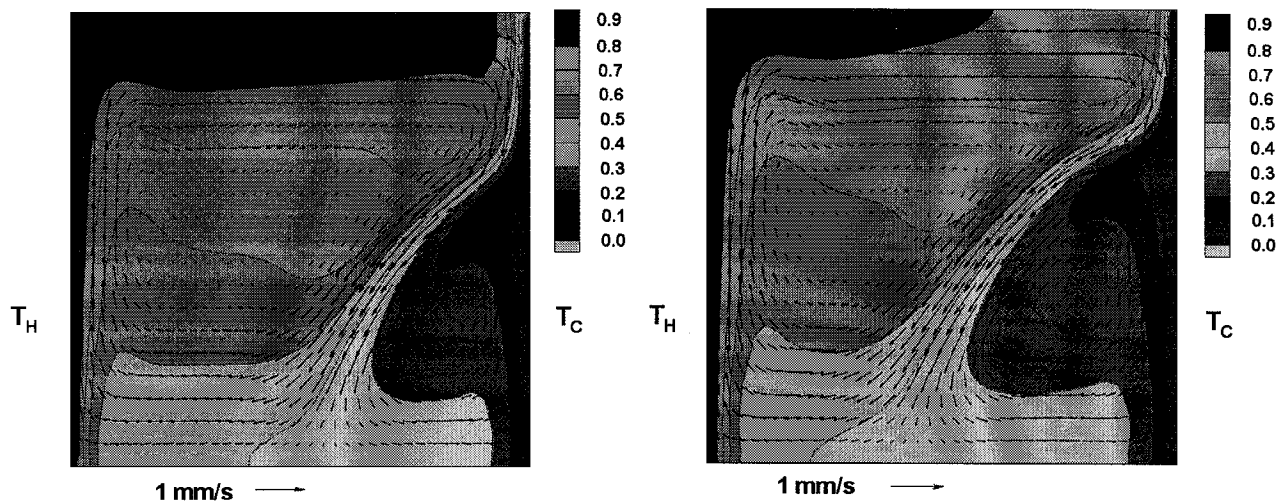


Figure 2. Steady-state free convection of water. Comparison of numerical solutions: left - boundary-fitted FDM (FRECON3V code<sup>12</sup>); right - operator-splitting FEM

*Alloy solidification with convection.* The results of calculations of the Al-alloy solidification with convection are given in Fig. 3, where stream-lines (with their values augmented  $10^5$  times) and isothermal lines are shown for the liquid Al-alloy confined in a square cavity (of 0.05m x 0.05m) and cooled from the initial temperature  $710^\circ\text{C}$  through the right cold wall, kept at temperature  $610^\circ\text{C}$  (the left wall temperature is equal to  $710^\circ\text{C}$ ). The volumetric liquid fraction and the fluid viscosity are assumed to be linear functions of temperature in the mushy zone (between  $625^\circ\text{C}$  and  $650^\circ\text{C}$ ). The results, received from calculations on the grid of 20x20 equal-order bi-linear elements, appear to be in agreement with the results reported by Usmani et al.<sup>1</sup>, obtained by using the simultaneous solution technique for the mixed FEM.

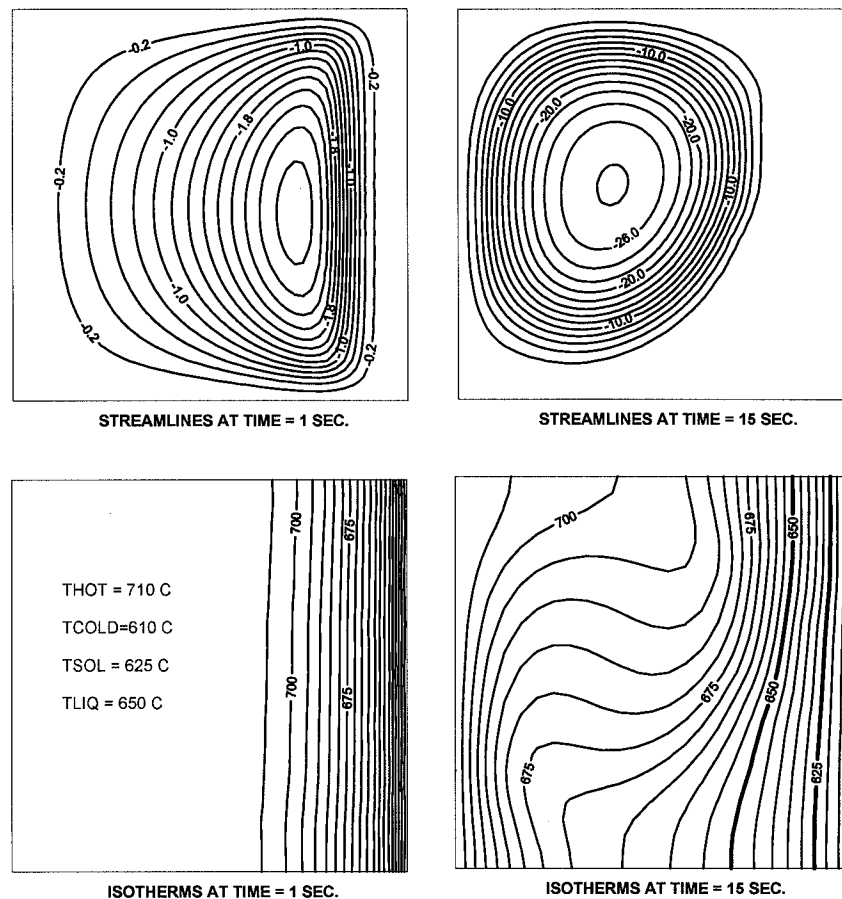


Figure 3. Streamlines and isotherms for Al-alloy solidification driven by conduction and convection

*Freezing of pure water.* A detailed analysis of performance of the presented algorithm is given for the challenging problem of freezing of water in the differentially heated square cavity. The temperature of the right-cold and the left-hot wall is set to  $-10^{\circ}\text{C}$  and  $+10^{\circ}\text{C}$ , respectively. The remaining cavity walls are assumed adiabatic. Freezing of water, unlike other natural-convection dominated phase change problems, is distinct due to the presence of density anomaly. Nonlinear temperature variation of water density, with its maximum at  $4^{\circ}\text{C}$ , creates a potential source of errors, when comparing physical and numerical experiments. Therefore, the results, obtained on the grid of  $40 \times 40$  equal-order bi-linear elements, have been carefully analyzed by comparing them with the experimental data<sup>8</sup>. The experiments have been performed in the cube shaped cavity. It is expected that effects of side walls are not negligible, and three-dimensional flow pattern develops. For comparison, however, the symmetry plane of the cavity is taken, assuming there nearly two-dimensional flow pattern. The numerical and experimental data are compared in Fig. 4, where velocity and temperature fields are given at two different times of freezing. At the first glance, the reliability of the proposed fixed grid FEM model appears to be „operationally” acceptable. The volume of solid created at the cold wall agrees quite well. However, the flow details and shape of the interface are far from good agreement. The computed interface close to the upper wall shows similar to observed cut-off. This is due to the relatively strong primary recirculation flow transporting hot liquid into the interface along left and top walls. However, in the numerical results this region is limited to about  $1/3$ th of the cavity height, whereas the one experimentally observed covers up to  $2/3$ th of the cavity. The lower part of the interface is almost perpendicular to the bottom wall, both in the numerical solution and experimental results. However, comparing the velocity field, comprehensive differences can be seen. The small recirculation of cold liquid, observed near the lower right corner, covers most of the cavity in the numerical simulation.

Hence, the cold water penetrates closer to the top of the cavity, effectively „squeezing” the hot recirculation. It is interesting to note that such immense change of the flow pattern has so little influence on shape of the interface.

Differences between numerical and experimental data can be explained by the limitation of the computational analysis to the two-dimensional flow approximation as well as by some freedom of definition of phase change region properties in the enthalpy-porosity approach. For example, the constant  $C_p$  in Eq.(5), that defines the morphology of the porous medium model, is arbitrarily taken as  $1.6 \times 10^6$ . Moreover, such effects like super-cooling, non-homogenous ice structure and non-adiabatic side walls, occurring in the real freezing, are not included in the numerical analysis. To get some insight, how far the numerical model itself is responsible for this incongruity, parallel computations have been performed using 3-D finite-difference code FREEZE3D, written by CFD Group at NSW University<sup>9</sup>. The boundary-fitted computational approach used in this code allows physically relevant description of the phase change front propagation. In the computations a very small time step is chosen to ensure smooth transition of the generated grid and the overall stability of the numerical calculations. First, the initial conditions have been compared. The „warm start” solution calculated by 3-D codes (both FREEZE3D<sup>9</sup> and FRECON3V<sup>12</sup>) deviates from the 2-D flow pattern obtained using the FEM code. Differences are not large, mainly limited to the recirculation at the bottom cold corner. The simplified 2-D simulation in FRECON3V code, that gives very similar 2-D flow pattern to the one resulting from the FEM calculations (Fig. 2), confirms that the initial differences, observed in the FEM solution and experimental data, are due to the 3-D effects. When the freezing starts and proceeds, the initial incompatibility between numerical and experimental results increases. The solution of the 3-D transformed grid model seems closer to the experimental findings, when the flow pattern is compared. But it evidently overestimates convective heat flux at the bottom part of the interface.

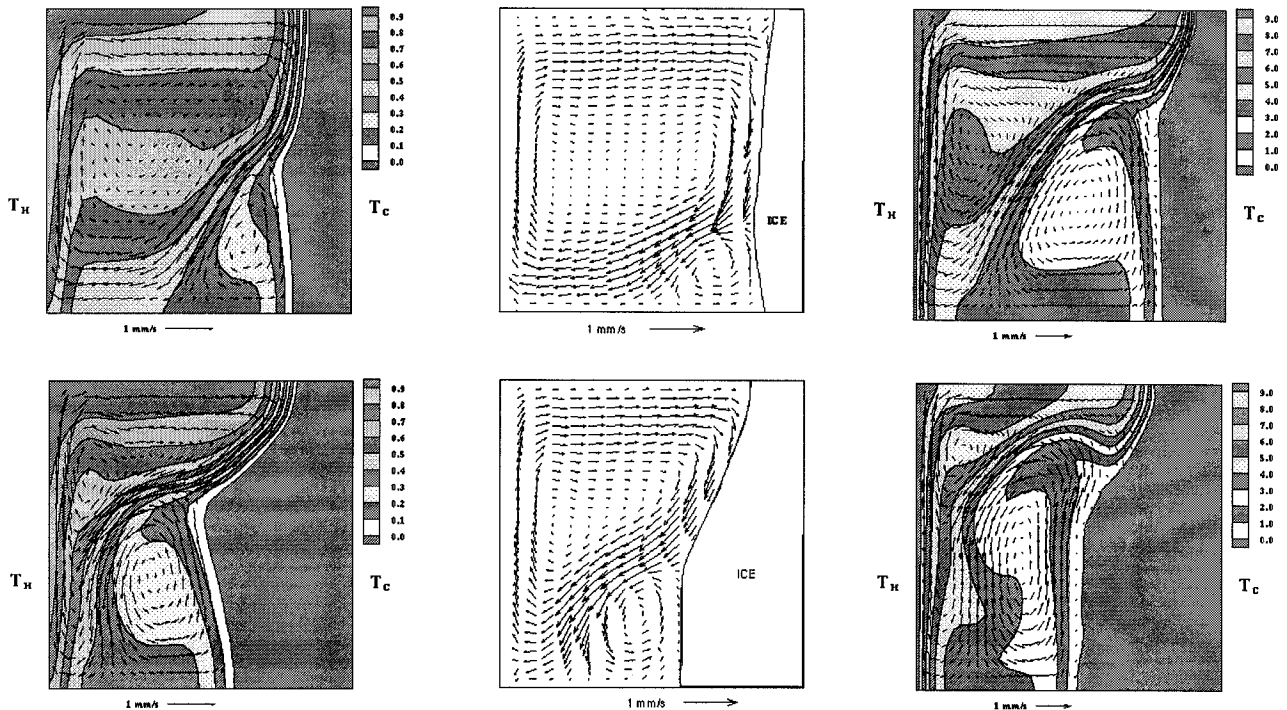


Figure 4. Comparison of flow pattern and temperature field for freezing of water in differentially heated cavity at time=500s. - the upper row and at time=3000s. - the lower row. Boundary fitted FDM - the left side, fixed grid FEM - the right side, experimental results - the central column

The fact, that visible discrepancies occur between experimental findings and both numerical solutions, that are obtained by using two completely different discretization techniques (front tracking FDM and fixed grid Galerkin FEM with the enthalpy-porosity model), does not allow to precisely answer the question of whether the fixed grid approach is sufficiently accurate for describing the constant temperature liquid-solid phase transition, driven by convection of a complex pattern (resulting from a non-linear temperature dependence of fluid density). Therefore, our further efforts are directed at developing the presented algorithm to three dimensional model and at searching for more precise description of the isothermal phase change on a fixed FEM grid.

### ACKNOWLEDGMENT

This work is supported by the National Committee for Scientific Research, grant Nr 3 T09C 002 12. The authors are indebted to G. de Vahl Davis and E. Leonardi (UNSW) for their computer codes FREEZE3D and FRECON3V.

### REFERENCES

1. Usmani, A.S., Lewis, R.W. and Seetharamu, K.N., Finite Element Modelling of Natural Convection - Controlled Change Phase, *Int. J. Num. Meth. in Fluids*, vol.14, 1992, pp 1019-1036.
2. Chorin, A. J., Numerical Solution of Navier-Stokes Equations, *Math. Comp.*, vol.22, 1968, pp 745 - 762.
3. Donea, J., Giuliani, A. S. and Quartapelle, L., Finite Element Solution of the Unsteady Navier-Stokes Equations by a Fractional Step Method, *Comp. Meth. Appl. Mech. Eng.*, vol.30, 1982, pp 53-73.
4. Ramaswamy, B., Jue, T. C., Some Recent Trends and Developments in Finite Element Analysis for Incompressible Thermal Flows, *Int. J. Num. Meth. Eng.* vol. 35, 1992, pp 675-692.
5. Patankar, S. V., *Numerical Heat Transfer and Fluid Flow*, Hemisphere Publ. Corp., NY,1980.
6. Voller, V. R. and Swaminathan, C. R., General Source-Based Method for Solidification Phase Change. *Numerical Heat Transfer*, Part B, vol.19, 1991, pp 175-189.
7. Brent, A. D. and Voller, V. R., Enthalpy-Porosity Technique for Modelling Convection-Diffusion Phase Change: Application to the Melting of a Pure Metal, *Numerical Heat Transfer*, vol.13, 1988, pp 297-318.
8. Kowalewski, T. A. and Rebow, M., An experimental benchmark for freezing water in the cubic cavity, *Proceedings of ISACHT'97*, Turkey, 1997.
9. Yeoh, G. H., Behnia, M., de Vahl Davis, G. and Leonardi E., A numerical study of three-dimensional natural convection during freezing of water, *Int. J. Num. Meth. Eng.* vol. 30, 1990, pp.899-914.
10. Kohlrausch, F., *Praktische Physik*, Band 3, 22 Auflage, Table 22203, p 1.692-1.693, B.G. Teubner Stuttgart, 1968.
11. Mallinson, G.D., de Vahl Davis, G. , Three-dimensional natural convection in a box: a numerical study, *J. Fluid Mech.*, vol. 83, pp 1-31, 1977.
12. Timchenko, V, Leonardi E. & de Vahl Davis, G., FRECON3V Users' manual, *Techn. Report 1997/FMT/1*, UNSW, Sydney 1997.